CAI REFRACTORY LITHOPHILE TRACE ELEMENT DISTRIBUTIONS: IMPLICATIONS FOR RADIOGENIC ISOTOPES. J. M. Paque[1], D. S. Burnett, J. R. Beckett and Y. Guan, Division of Geological and Planetary Sciences, California Institute of Technology, Pasadena, CA 91125, [1]jheather@gps.caltech.edu.

Introduction: Concentrations of refractory lithophile elements (**RLE**) in Allende Type B1 CAI melilite do not agree with expectations from the fractional crystallization (**FC**) processes which formed these objects [1-4]. Part of the discrepancy reflects inclusions (possibly relict grains that predate the CAI itself). The analyzed volume for a typical SIMS analyses of melilite in the Type B1 CAI Leoville 3537-2 [**LV**; 5-6] incorporates enough included material to cause the measured concentrations for most elements to be high relative to FC predictions. Clinopyroxene and perovskite inclusions have been identified by SEM observation and RLE abundance patterns [7]. Where inclusions are depth resolved in ion probe profiles, we can filter out their contributions, permitting a direct comparison between filtered residuals (ideally melilite only) and FC predictions.

Analyses: The Zinner-Crozaz energy offset technique was adapted to the Caltech Cameca 7f Geo ion microprobe. Two standards were used: an $Åk_{40}$ melilite glass (for Sc and Be) and a CAI Type B bulk composition glass doped with Sr, Y, and Ti at levels analyzable by electron probe (nominal 1000 ppm). Each analyzed spot contains 40 slices approximately 40 µm in diameter by 0.1 µm deep. The data were examined in terms of trends as a function of depth within a spot, and spot to spot variations.

Data Processing: Ti profiles were examined for peaks indicative of submicron inclusions. In 11 profiles, a clear inclusion peak is superimposed on a relatively flat background (Fig. 1a); after removing the peak, the remaining inclusion filtered (**IF**) average concentration is taken to be inclusion free melilite. In 30 spots, a flat region was not observed (Fig. 1b); we took RLE concentrations in the slice with the *lowest* Ti as upper limits for the melilite.

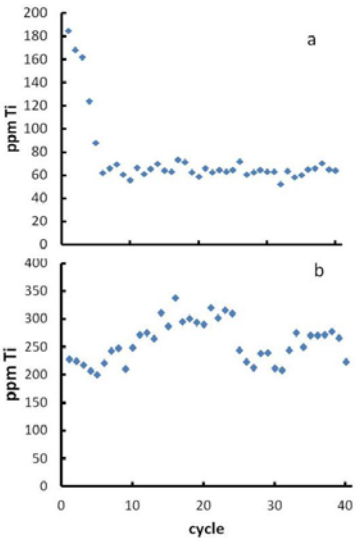

Figure 1. Ti profiles for 2 spots: (a) shows flat area with no evidence of inclusions, and in (b) inclusions predominate.

Results: Figure 2 compares filtered (nominally inclusion free melilite) concentrations for five RLE with FC predictions as a function of Åk. Both core and mantle data are included. Mantle melilite formed after spinel, and represents FC dominated by a single phase; this, plus measured partition coefficients (D) [9], permits accurate FC predictions. Inclusion core data demonstrate systematics in the RLE data over an extended Åk range, but are complicated by remelting following initial crystallization [8] and co-crystallization of melilite with clinopyroxene and anorthite, making FC modeling uncertain. We therefore truncate FC calculations at ~$Åk_{40}$.

Fig. 2 highlights the IF concentrations (red squares), which are our best estimate of melilite RLE

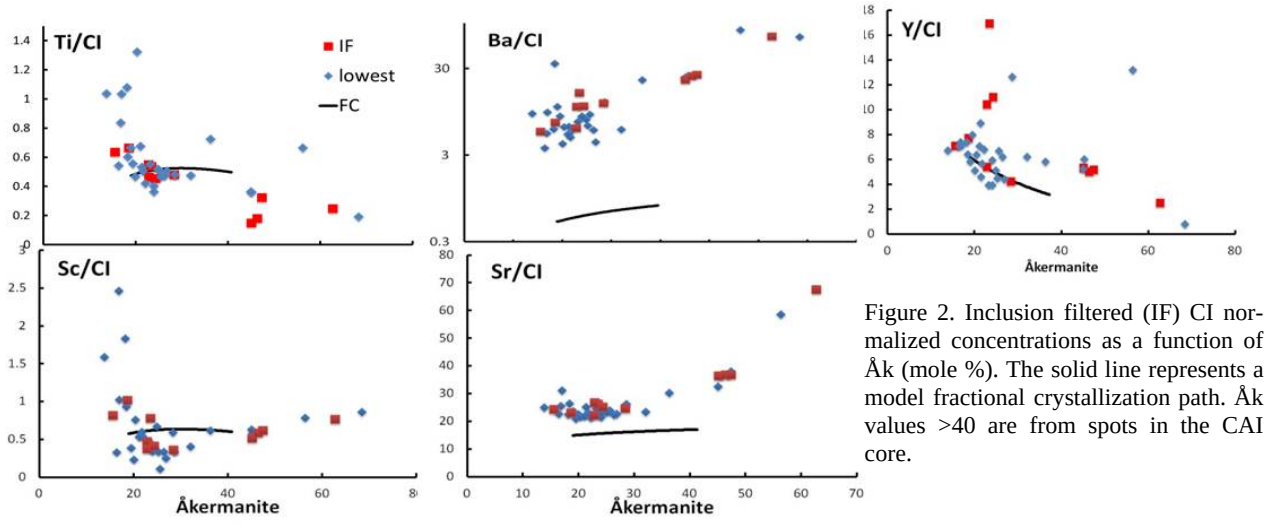

Figure 2. Inclusion filtered (IF) CI normalized concentrations as a function of Åk (mole %). The solid line represents a model fractional crystallization path. Åk values >40 are from spots in the CAI core.

concentrations. For FC, the IF should show a smooth trend with Åk. FC predictions should match this trend, but this is less important than the existence of a smooth trend. Further, the lowest Ti concentrations should either agree with or be above the IF trend.

Of the many interesting features in Fig. 2, we highlight a few. Overall, for Ti, Y, and Sc, there is reasonable agreement between the FC predictions for much of the mantle melilite. Smooth curves for IF data are best illustrated by Sr and Ba, which show strongly increasing concentrations between mantle and core, apparently reflecting incompatibility in all crystallizing phases. However, as recognized previously [3], the concentrations of Sr, and especially Ba, are much higher than expected from FC. Observed clinopyroxene and perovskite inclusions have modest concentrations of Ba and Sr, so filtering out the effects of Ti-rich inclusions does not resolve the discrepancies, possibly indicating that there are sub-100 nm Sr and, especially, Ba-rich inclusions that dominate the concentrations of these elements.

The IF trends for Ti, Sc, and Y are not smooth, suggesting that the apparently flat regions of the Ti profiles still contain inclusion contributions for Ti, Sc, and Y, or that the melt from which melilite crystallized was heterogeneous (e.g., dominated by dissolving inclusions and/or melt that did not homogenize on the time scale of crystallization). The Ti FC prediction is based on D(Ti) measured in a CCO experiment for $Åk_{20\text{-}25}$ melilite, scaled to an Åk dependence based on Sc, which decreases with Åk. A decrease in D coupled with uptake of Ti and Y in core clinopyroxene causes the overall mantle to core decrease in Ti and Y. Points below the IF points may reflect Ti and Y (i.e., inclusion) depleted melt.

Be profiles show no evidence for inclusions and show no correlation with Ti or with any other element. Filtered Be concentrations agree with the spot averages; therefore, all data in a spot (which has much higher precision than an individual slice) are plotted in Fig. 3. Be in Type B1 CAIs is totally decoupled from other RLE. The smoothness of the Åk trend in Fig. 3 is best interpreted as a pure FC trend.

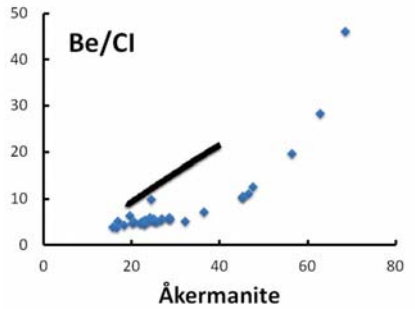

Figure 3. Be as a function of Åk. Model fractional crystallization is represented by the solid line.

Implications for Be isotope chronology. The majority of the radiogenic isotope systems relevant to CAIs involve RLE. The fact that many parent-daughter elements are located in inclusions, possibly relict grains, affects the interpretation of radiogenic isotope data. Consider ^{10}Be and ^{7}Be. Whatever Be carriers were present in the solids that were melted to produce LV were apparently sufficiently soluble to dissolve readily in the initial liquid and the resulting Be distribution is controlled by partitioning behavior. This is a favorable situation for chronology in that the daughter isotopes are produced in a regular crystalline environment, in LV an environment free from the pervasive secondary alteration found in Allende CAIs. The strong enhancement of Be in the CAI core melilite indicates that core melilite should have the most radiogenic enrichments in ^{10}B or ^{7}Li.

A smooth trend of Be concentration with Åk is expected for FC equilibrium partitioning. Our model FC curve for mantle melilite lies above the data, but this is a separate problem. Be is a moderately compatible element in melilite (D=0.45 at $Åk_{20}$) with D increasing with Åk (about 0.9 at $Åk_{40}$) [9] This explains the observed strongly increasing trend of Be with Åk. Within mantle melilite, where the model should be valid, the variation is less steep than predicted. At $Åk_{30}$ the difference between the measured and model Be differ by >2x. It is unlikely that analytical errors in the measurement of LV concentrations or in the partition coefficients can explain this difference, especially since the same Be standard was used in both measurements. The FC model assumes that the initial whole CAI Be concentration was 18.5xCI; it could be lower but the difference in slope would remain.

To determine ^{7}Be-^{7}Li isochrons, Chaussidon et al [10] proposed that "unperturbed" melilite analyses could be selected as those matching the Be concentration with Åk trend expected from [9]. Our results support an FC origin for Be but not the predicted FC Åk trend. Our LV inclusion would meet the criterion of [10]; however Li isotope data [7] show no evidence for ^{7}Be.

References: [1] Davis A. M. et al. (1992) *LPS XXIII*, 281-281. [2] Simon S. B. et al. (1996) *LPS XXVII*, 1201-1202. [3] Davis A. M. et al. (1996) *LPS XXVII*, 291-292. [4] Kennedy A. K. et al. (1997) *GCA 61*, 1541-1561. [5] Paque J. M. et al. (2011) 42nd LPSC, 2096. [6] Paque J. M. et al. (2011) Formation of First Solids in the Solar System, 9087. [7] Burnett D. S. et al. (2012) 43rd LPSC, 2159. [8] Beckett J. R. et al. (2000) GCA 64, 2519-2534. [9] Beckett J. R. et al. (1990) GCA 54, 1755-1774. [10] Chaussidon M. et al. (2006) GCA, 70, 224–245.